DALTON
FULL PAPER

Self-assembled organoplatinum(II) supermolecules as crystalline, SO_2 gas-triggered switches †

Martin Albrecht,[a] Martin Lutz,[b] Antoine M. M. Schreurs,[b] Egbert T. H. Lutz,‡[c] Anthony L. Spek §[b] and Gerard van Koten *[a]

[a] *Debye Institute, Department of Metal-Mediated Synthesis, Utrecht University, Padualaan 8, 3584 CH Utrecht, The Netherlands. E-mail: g.vankoten@chem.uu.nl; Fax: +31-30252-3615*
[b] *Bijvoet Center for Biomolecular Research, Crystal and Structural Chemistry, Utrecht University, Padualaan 8, 3584 CH Utrecht, The Netherlands. E-mail: a.l.spek@chem.uu.nl*
[c] *Department of Vibrational Spectroscopy, Utrecht University, Sorbonnelaan 16, 3584 CA Utrecht, The Netherlands*

First published as an Advance Article on the web 26th September 2000

Square-planar platinum(II) complexes containing N,C,N terdentate coordinating, anionic 'pincer' ligands reversibly bind gaseous SO_2 in the solid state by Pt–S bond formation and cleavage giving five-coordinate adducts. When the starting material is crystalline, exposure to this gas leads to quantitative adduct formation with the unique feature that the product is also crystalline, although the crystal structures of the adduct and the SO_2 free complex are significantly different from each other and are both non-porous. Remarkably, the reverse reaction, *i.e.* the release of SO_2 gas, modifies but does not destroy the crystalline ordering in the arylplatinum assemblies. These processes include repetitive expansion and reduction of the crystal lattice without any loss of crystallinity of the material. Variation of the ligand framework revealed that the presence of intermolecular interactions such as α- or β-type networks is not an essential prerequisite for these crystalline transformations. Consequently, this class of supermolecules provides access to sensitive crystalline switches with 'on' and 'off' positions which are a direct response to the gaseous environment.

Introduction

A considerable amount of research in materials science is currently devoted to the downsizing of operational devices to nanosize processing units composed of a well-defined (small) number of molecules.[1] For most applications (*e.g.*, (opto-)electronics, molecular machines[2]), an ideal ordering and high molecular regularity of such materials is beneficial and sometimes even essential. Tailored crystalline devices would be excellent systems for these purposes, since crystals are supermolecules with a perfectly ordered structure throughout a vast number of self-assembled molecules.[3] A critical issue in crystal engineering, the property-directed design, synthesis and processing of crystalline solids,[4] is the prediction of general trends and principles of the crystallisation process and hence the design of crystal structures rather than molecular entities. The possibility of translating a rational molecular design into *inter*molecular architectures would be highly desirable, since this would allow the selection of macroscopic materials properties on a molecular level. Whereas excellent computational models have been developed for the calculation of the shape or geometry of a single molecule,[5] advances in the prediction of its packing properties and hence the crystal structure have proceeded with only a limited amount of success.[6] Illustrative examples which emphasise this are the structure(s) of higher-order cyanocuprates[7] and the phenomenon of polymorphism.[8]

A versatile methodology to overcome these limitations consists of a controlled self-assembly of molecular building blocks in the solid-state, induced by weak non-covalent forces.[4,9] Empirical studies have shown that the formation of supramolecular structures is promoted by the recognition of distinct sites of molecular unit(s), predominantly based on electrostatic interactions (hydrogen bonding, cation/anion interactions, π-stacking).[10] The presence of such key building blocks with intermolecular interactions, *i.e.* supramolecular synthons, may direct the crystallisation process. An extension of this concept for crystal engineering[11] comprises the selective and direct chemical modification of structurally characterised crystals. So far, such so-called 'crystalline-state reactions'[12] have been limited mainly to 'open', *i.e.* porous structures[13] that contain large, solvent accessible cavities (*e.g.*, enzymes,[14] zeolites[15]). In closed crystal structures, however, a supermolecule is densely packed and it is generally anticipated that any change (*i.e.*, any reaction) in the single molecule would cause considerable stress and consequently destroy the supermolecule and its properties, irreversibly in most cases. Among the best explored crystalline-state reactions in closed structures are (reversible) mono- or bi-molecular photochemical isomerisation processes, *i.e.*, light-induced transformations that do not change the overall atom content of the crystal.[16]

Our approach towards the synthesis and processing of new and well-defined crystalline materials[17] involves the coordination of the terdentate, meridionally coordinating monoanionic 'pincer' ligand system[18] $[C_6H_2(CH_2NMe_2)_2$-2,6-R-4$]^-$ (abbreviated as NCN–R) to a d^8 metal centre (*e.g.*, Pd^{II}, Pt^{II}), which leaves a fourth coordination site for a ligand to bind selectively *trans* to C_{ipso} (Scheme 1). Suitable modification of the NCN-aryl ring in the *para*-position, and proper choice of the additional monodentate ligand leads to a planar molecule with

† Based on the presentation given at Dalton Discussion No. 3, 9–11th September 2000, University of Bologna, Italy.

Electronic supplementary information (ESI) available: rotatable 3-D crystal structure diagram in CHIME format. See http://www.rsc.org/suppdata/dt/b0/b006419j/

‡ Deceased on May 20, 1999.

§ Corresponding author pertaining to crystallographic details.

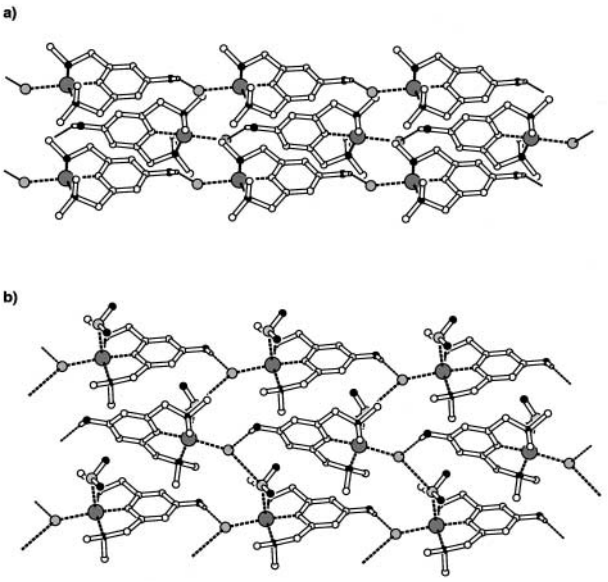

Fig. 1 Crystal structures of the organoplatinum complexes **1** and **2**. The α-type supramolecular connectivity pattern, *i.e.*, the Pt–Cl · · · H–O hydrogen bonding, is similarly present in **1** (a) and in **2** (b). The β-type network mediated by Pt · · · S(O)$_2$ · · · Cl interactions is only found in **2**. All hydrogen atoms except the phenolic O–H hydrogen have been omitted for clarity.

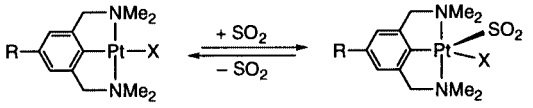

1	R = OH, X = Cl	**2**
3	R = H, X = Cl	**6**
4	Br	**7**
5	I	**8**

Scheme 1 Reversible binding of SO_2 by arylplatinum(II) species containing the N,C,N′ terdentate coordinating 'pincer' ligand.

directional, linearly arranged acceptor and donor sites. This concept is illustrated by the development of the arylplatinum complex [PtCl(C$_6$H$_2${CH$_2$NMe$_2$}$_2$-2,6-OH-4)] **1**,[19] which contains a metal-bound chloride as a potential hydrogen bonding acceptor and a phenolic hydroxide group on the pincer ligands as a potential donor unit. Consequently, **1** self-assembles in the solid-state to form an α-type network through O–H · · · Cl–Pt hydrogen bonding (Fig. 1a), a relatively strong and highly directional class of interactions.[20]

Only recently, the corresponding sulfur dioxide complex, [PtCl(NCN–OH)(SO$_2$)] **2** has been characterised (Scheme 1).[21] When compared to SO_2-free **1**, the structural features of this complex are significantly changed in the unit cell (*e.g.*, in volume) as well as in the molecular structure, since the η^1-*S*-coordinated SO_2 molecule changes the geometry around the platinum centre from square-planar to square-pyramidal. Surprisingly however, this complex shows *supra*molecular properties that are identical to those of the parent complex (Fig. 1b). For example, the O–H · · · Cl–Pt donor–acceptor distance and the hydrogen bond angle are statistically identical (distance O · · · Cl: 2.32(13) Å in **1** *vs.* 2.33(9) Å in **2**; angle O–H · · · Cl: 161(15)° in **1** *vs.* 165(8)° in **2**). These striking similarities prompted us to investigate the reactivity of such arylplatinum complexes with SO_2 in more detail, a study that resulted in the discovery of the solid-state reaction of closed structures, in which the starting material and the product are crystalline although the overall atom content of the unit cell is changed during the reaction.[22] Here, we report on this transformation and on our studies towards its scope and limitations.

Results and discussion

Solid-state reactivity of crystalline 1 and 2

When colourless crystalline [PtCl(NCN–OH)] **1** is subjected to an atmosphere containing gaseous SO_2 (1 atm), a fast reaction takes place affording the corresponding bright orange adduct [PtCl(NCN–OH)(SO$_2$)], **2** (Scheme 1) also as crystalline material in a quantitative, solid-state reaction. Unequivocal evidence for this unique process has been obtained from powder X-ray diffraction measurements. The interpretation of these experiments has been considerably facilitated since the data from the single crystal structure determinations are available for both complexes **1** and **2**. Hence, analysis of the obtained diffractogram is easily accomplished by comparison with the expected pattern calculated from the single crystal data.

Exposure of crystalline **1** to gaseous SO_2 for *ca.* 1 minute is sufficient to ensure complete conversion to **2**. This is clearly indicated by the presence of a completely new powder pattern in the X-ray diffractogram of the product, assigned to **2**, whilst all peaks originating from **1** were absent. Short exposure time of **1** to SO_2 leads to a more complicated diffraction pattern, which has been interpreted as a superposition of the expected patterns of isolated **1** and **2**, respectively. This is in agreement with partial conversion only. When this mixture is subjected to an atmosphere of SO_2 for a prolonged time, the diffractogram indeed simplifies and ultimately, only the set corresponding to the SO_2 adduct **2** is observed. The ratio between **1** and **2** in any mixture is readily identified, however, by analysing the diagnostic peaks. In particular the diffractions at $2\theta = 13.35°$ and 11.33° ($\lambda = 1.5418$ Å) are very pronounced in the adduct **2** and the SO_2-free material **1**, respectively, and are entirely absent in the other complex.

This solid-state reaction involves the transition of a crystalline, closed structure into another one, which is still densely packed but which has a different structure and atomic content. This implies an expansion of the volume of the unit cell by more than 15% and a change of the crystal structure. Remarkably, in these arylplatinum materials this occurs in a very controlled process that modifies the crystalline organisation without any destructive consequences.

Reversibility of this selective and distinct inclusion of SO_2 into these arylplatinum structures is indicated by exposing a sample of **2** to air. After only a few minutes, a significant increase in the intensity of 11.33° unambiguously demonstrates an enhanced concentration of **1**, and after 10 h, the SO_2-free starting material **1** is fully recovered. Such gas absorption—desorption cycles, *i.e.*, the reversible switching between crystalline **1** and **2**, have been repeated several times without any notable loss of crystallinity or activity. These processes involve a remarkable expansion and shrinking of the crystalline material (*cf.* unit cell dimensions of **1** and **2**).[23] On a molecular level, these transformations correspond—besides others—to the repetitive β-type network formation and cleavage process, which is defined by successive making and breaking of Pt · · · S(O)$_2$ · · · Cl interactions. Consequently, these materials may work as crystalline switches[24] that are triggered by the SO_2 content of the (micro-)environment. The current position of these switches (on or off) may be identified by various techniques such as *in situ* IR (ν_s of metal-bound SO_2 as a versatile probe), by X-ray diffraction techniques or by monitoring the transparency properties (*e.g.*, solid-state UV-vis).

Since the gas fixation is fast and complete in less than 1 minute, X-ray diffraction does not allow for detailed investigation of this process. An independent technique is provided by time-resolved solid-state infrared (IR) spectroscopy. For this purpose, a sample of crystalline **1** was mixed with powdered CaF_2 and placed without further treatments into a stream of SO_2.[25] Continuous monitoring of the IR absorbance spectra then visualises the course of the gas fixation process. The range between 1000 and 1400 cm^{-1} is diagnostic, since in this region

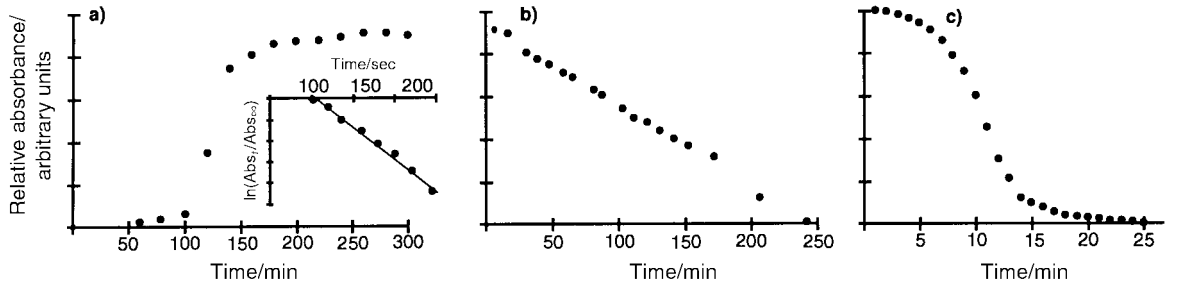

Fig. 2 Time-dependent increase of the IR absorbance of the metal-bound SO_2 vibration at $\nu_s = 1073$ cm^{-1} (a) upon exposure of **1** to an atmosphere of pure SO_2. The inset shows a logarithmic plot of the changes in absorbance related to the elapsed time (correlation >0.995 for a linear approximation). The initial 80 seconds have been ignored in this analysis, see text for further details. A change of the environment to air leads to a decrease in this absorption band, which has been monitored (b) at ambient (293 K) and (c) at elevated temperature (333 K).

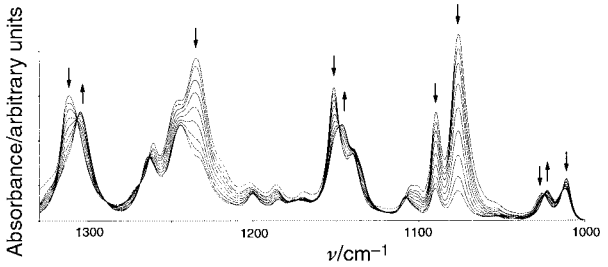

Fig. 3 The overlapping IR spectra (absorbance) for the SO_2 desorption reaction, shown in the characteristic range between 1330 and 1000 cm^{-1}, display a series of isosbestic points. Spectra are shown after exposure of **2** to air (time interval is 30 min) and the spectrum recorded after 4 h is identical to that of **1**.

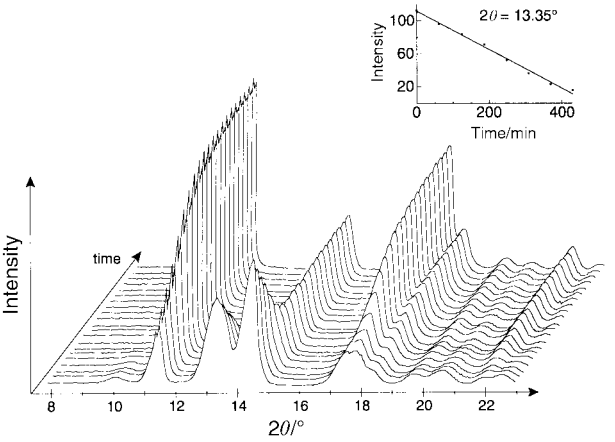

Fig. 4 Time-resolved powder X-ray diffractograms of **2** exposed to air. Diffraction patterns are shown after every hour. The change of the intensity signals at $2\theta = 13.35°$ (characteristic for the presence of **2**) and at $2\theta = 11.33°$ (for **1**) are diagnostic for a unique process where both starting material and product are crystalline.

the characteristic stretching vibrations of metal-bound SO_2 in adduct **2** are expected to appear ($\nu_s = 1073$ cm^{-1}, $\nu_{as} = 1236$ cm^{-1}).[21,26] A typical reaction profile for the formation of adduct **2** (from solid **1** in an atmosphere of pure SO_2) has been obtained by monitoring the absorption activity of the reaction mixture at $\nu = 1073$ cm^{-1} (Fig. 2a). Saturation of the measuring compartment with SO_2 prior to the reaction of the gas with crystalline **1** is reflected by the fact that in the initial 80 seconds of monitoring, no relevant changes have been observed in the IR absorption spectrum. Detailed examination of the subsequently measured data points reveals a rate law which is best approximated by pseudo-first-order reaction kinetics in platinum ($k = 2.52(27)\ 10^{-2}$ s^{-1}, see inset Fig. 2a). This value represents a reliable rate constant measured for the binding of SO_2 gas in a crystalline material at ambient pressure. Note that the exact value of the rate constant for the formation of **2** is strongly influenced by the surface constitution of the solid material: with finely crunched powders, binding of SO_2 occurs faster than with single crystals of millimeter-size dimensions.

The SO_2 release, *i.e.*, the solid-state reaction of **2** to form **1** is much slower at room temperature than the reverse transformation and may therefore be investigated by a variety of techniques. Monitoring the gas release by IR spectroscopy has shown a gradual transformation of **2** to **1** and no detectable amount of an eventually formed intermediate has been observed. A typical plot of the overlapping spectra of this transformation sequence is shown in Fig. 3 and demonstrates a few important aspects: first, the reaction clearly occurs inside the crystalline material and not only on its surface (baseline modifications) and second, a series of isosbestic points strongly indicates an equilibrium reaction between two species, *viz.* **1** and **2**. When a sample of **2** is stored under an inert gas atmosphere (N_2), a linear decrease of the absorption bands due to metal-bound SO_2 is observed, which is in accordance with a gradual transformation of **2** into the SO_2-free complex **1** (Fig. 2b). After 4 h, no residual **2** was detected, thus indicating the completion of the reaction. Importantly, the rate of this process can be decreased by performing the reaction at lower temperatures. At 253 K, for example, the reaction has not reached 50% conversion even after 5 days. At more elevated temperatures (333 K), however, the reaction is accelerated as **1** is detected exclusively after only 0.5 h (Fig. 2c). It is noteworthy, that the reaction profile (and hence presumably also the mechanism) of this high temperature process is not linear anymore and therefore differs significantly from the one observed at ambient temperature.

Time-resolved powder X-ray diffraction measurements[27] revealed qualitatively similar results as observed with IR spectroscopy. The decrease of the signal intensities due to crystalline adduct **2** is accompanied by a proportional increase of the intensities originating from **1** (Fig. 4). The reaction in a thin glass capillary is, however, considerably slower than in an open cup (IR) and has reached completion after *ca.* 8 h. Analysis of the characteristic intensities at low 2θ values strongly suggests a linear relationship between the change of the intensities and the elapsed time (see inset Fig. 4). Hence, a zero-order rate law is deduced for the release of gas from crystalline **2**. The exact reaction rate is strongly dependent on various properties of the sample surface (*e.g.*, particle size, packing of the material). Similarly, the release of this gas from single crystals of **2** is complete only after *ca.* 2 days (*cf.* 8 h in material suitable for powder X-ray diffraction). This is most likely a direct effect of the smaller surface area in single crystals compared to (micro)-crystalline powder (approximate ratio $1:10^3$). When SO_2-free **1** is generated from single crystals of **2**, the shape of the material is kept even though the crystal is not suitable for a single crystal structure analysis anymore. When such a 'crystal' is mounted on a diffractometer, no distinct reflections have been detected and only powder diffraction patterns are observed.

Microscopy studies have finally demonstrated that the loss of SO_2 from single crystals of **2**, which are stored in air,

Table 1 Selected crystallographic parameters of **1**–**8**

Complex (R, X)	Space group (No.)	Z	Unit cell parameters					Filled space (%)[f]
			a/Å	b/Å	c/Å	β/°	V/Å^3	
1 (OH, Cl)[a]	$Pna2_1$ (33)	4	24.2238(14)	10.1986(8)	5.4483(14)		1346.0(4)	72.2
2 (OH, Cl)[b]	$Pna2_1$ (33)	4	16.837(3)	10.2189(16)	9.0231(10)		1552.5(4)	70.9
3 (H, Cl)	$P2_1/c$ (14)	4	12.9877(14)	9.2177(6)	11.6041(12)	111.104(8)	1296.0(2)	72.5
4 (H, Br)[c]	$P2_1/c$ (14)	4	12.630(7)	9.846(4)	11.742(3)	110.61(2)	1366.7(9)	70.2
5 (H, I)[d]	$I2/a$ (15)	8	17.044(6)	9.259(3)	18.44(1)	96.65(4)	2890(2)	67.8
6 (H, Cl)	$Pna2_1$ (33)	4	16.7796(1)	10.0141(1)	9.0940(1)		1528.09(2)	70.3
7 (H, Br)[e]	$P2_1$/c (14)	4	14.215(1)	9.840(1)	11.895(1)	113.15(1)	1541.4(5)	64.2
8 (H, I)	$Pbca$ (61)	8	8.0291(9)	15.1212(13)	25.985(4)		3154.8(7)	70.5

[a] From ref. 19. [b] From ref. 21. [c] From ref. 28. [d] From ref. 29. [e] From ref. 30. [f] Calculated by the routine CALC VOID as implemented in PLATON (ref. 43).

predominantly occurs at the crystal surface. This results in crystalline material that is coloured orange in the core but colourless at the periphery.[22] Upon prolonged exposure of such crystals to air, the colourless zone slowly expands and grows towards the core until finally, no orange domains are present anymore. At this point, the conversion of **2** to crystalline **1** is complete. These results provide another indication for a desorption process in the crystalline material which is fast at the surface.

Modifications in the arylplatinum complexes

It might be argued that weak intermolecular interactions stabilise the crystallinity of these materials during the reaction with SO_2. Therefore, it seemed interesting to us to see whether the presence of a supramolecular motif, *e.g.*, an α- or β-type network, is an essential prerequisite for these reversible expansion–shrinking processes. For this purpose, the synthons that predominantly induce the self assembly of **1** or **2** in the solid state, *i.e.*, the hydrogen bond donor and acceptor sites, have been modified. In particular, the metal-bound halide X and the nature of the substituent R (X = Cl, Br, I; R = OH, H) have been varied, thus affording a series of arylplatinum complexes **3**–**5** for organometallic crystal engineering (Scheme 1). The preparation of these complexes and of the corresponding SO_2 adducts **6**–**8** has been described previously[21] and the crystal structures of some of these have been reported.[28–30] The parameters from the single crystal X-ray structures facilitate the interpretation of the results from powder X-ray diffraction measurements considerably. Therefore, the so far unknown solid-state structures of the arylplatinum(II) complex **3** (X = Cl), and of the SO_2 adducts **6** (X = Cl), and **8** (X = I) have been determined prior to the examination of their reactivity in the crystalline state.

Single crystal X-ray structures of arylplatinum complexes with R = H, and their SO_2 adducts

Complex **3** crystallises in space group $P2_1/c$ (Table 1). The molecular structure (Fig. 5a) shows the typical features developed earlier for platinum(II) complexes containing the terdentate coordinating anionic pincer ligand.[18,28–31] The metal centre adopts a distorted square-planar geometry and is held in a rigid position by the bis(*ortho*-)chelating ligand (Pt–C(1) 1.907(5) Å; Table 2). Consequently, the chloride ion which occupies the fourth coordination site, is forced into a mutual *trans* position with respect to the metal-bound carbon (θ(C(1)–Pt–Cl) 177.1(1)°). The two five-membered metallacycles are puckered, which is reflected by a dihedral angle of the platinum coordination plane with the aryl plane of 12.4(11)°. These structural properties closely relate the chloride-containing complex **3** to complexes **4** and **5** containing different metal-bound halide ions, which display similar features with the exception of the different metal–halide bond lengths.[32]

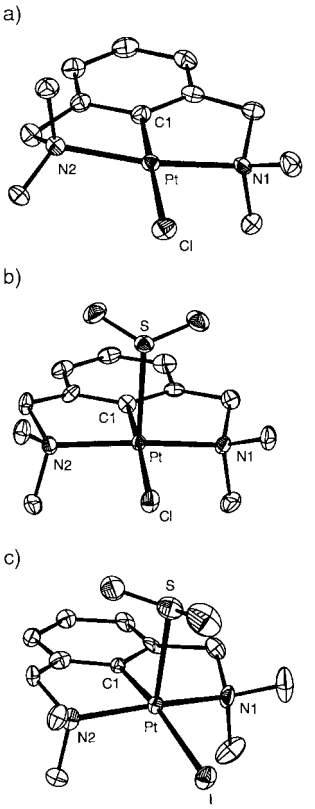

Fig. 5 Perspective view (50% probability) of the molecular structures of (a) the square-planar arylplatinum complex **3** containing a metal-bound chloride; (b) of the corresponding SO_2 adduct **6**; (c) of the analogous square-pyramid SO_2 adduct **8** containing a metal-bound iodide.

In the corresponding SO_2 adducts **6** and **8** (Fig. 5b and c), the penta-coordinated platinum centre possesses a square-pyramidal ligand arrangement, whose basal points are formed by the N,C,N′ donor system of the pincer ligand and the halide ion. Consequently, the approximately linear arrangement of the C(1)–Pt–X fragment from the SO_2-free complexes is further distorted (θ 169.4–173.3° in **6**–**8**; Table 2)[29] and the *trans* influence is weakened. The SO_2 molecule occupies the pseudo-apical position and is connected to the platinum centre in an η^1-Pt–S bonding mode. The different platinum–sulfur bond lengths (Pt–S 2.570(1) Å in **6** with X = Cl, 2.613(7) Å in **7** with X = Br, and 2.512(3) Å in **8** with X = I) established in the solid-states of the adducts **6**–**8** seem unusual at a first glance. It may be rationalised, however, by considering the detailed bonding principles of SO_2 to d^8 transition metals,[26] which are affected by the combination of π acceptor and donor influences of the pincer ligand and the metal-bound halide. Note that in the present cases, the major interaction of the Pt–S bond is a metal-to-ligand charge transfer and therefore represents another

Table 2 Relevant bond lengths (Å) and angles (°) in the arylplatinum(II) complexes (**1**, **3**–**5**) and their SO_2 adducts (**2**, **6**–**8**)

	1[a] (X = Cl)	2[b] (X = Cl)	3 (X = Cl)	4[c] (X = Br)	5[d] (X = I)	6 (X = Cl)	7[e] (X = Br)	8 (X = I)
Pt–C(1)	1.915(9)	1.923(10)	1.907(5)	1.90(1)	1.933(6)	1.934(4)	1.96(1)	1.945(8)
Pt–N1	2.094(8)	2.106(8)	2.083(3)	2.09(1)	2.099(5)	2.096(3)	2.10(1)	2.106(7)
Pt–N2	2.082(8)	2.094(8)	2.088(3)	2.07(1)	2.087(5)	2.094(3)	2.09(1)	2.097(7)
Pt–X	2.434(2)	2.423(3)	2.407(1)	2.526(2)	2.716(2)	2.409(1)	2.522(7)	2.7253(8)
Pt–S	—	2.531(3)	—	—	—	2.570(1)	2.613(7)	2.512(3)
C(1)–Pt–X	177.4(4)	173.1(3)	177.05(12)	177.4(4)	179.6(2)	173.14(11)	173.3(4)	169.4(2)
C(1)–Pt–N1	81.6(4)	82.3(4)	82.04(16)	82.9(5)	81.8(2)	83.32(13)	82.8(5)	82.2(3)
C(1)–Pt–N2	82.4(4)	81.5(4)	82.22(16)	81.5(5)	81.6(2)	81.95(13)	81.7(5)	81.5(3)
N1–Pt–N2	163.9(3)	160.5(3)	164.26(13)	164.4(4)	163.4(2)	161.27(12)	160.4(5)	158.9(3)
C(1)–Pt–S	—	90.0(3)	—	—	—	88.45(11)	84.5(5)	87.3(2)
X–Pt–S	—	96.9(1)	—	—	—	98.28(3)	102.2(2)	103.3(1)

[a] From ref. 19. [b] From ref. 21. [c] From ref. 28. [d] From ref. 29. [e] From ref. 30.

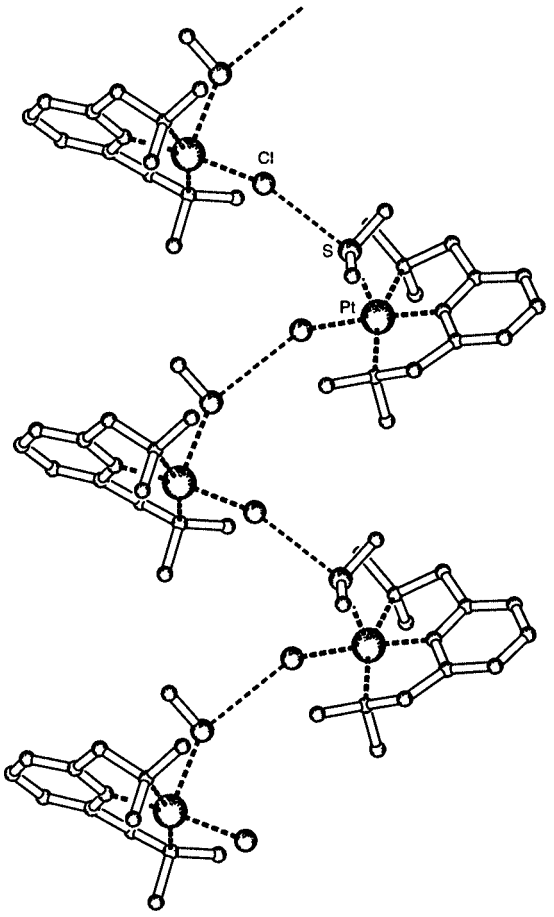

Fig. 6 Intermolecular connectivities in the crystal structure of **6** demonstrating the presence of a $Pt\cdots S(O)_2\cdots Cl$ mediated α-type network.

indication for the enhanced nucleophilicity of the platinum(II) centre when bound to a pincer-type framework.[21,33]

Interestingly, in the crystal structure of **6**, close contacts of the SO_2 molecule are observed not only to the platinum centre but as well to a chlorine ion of an adjacent molecule of **6** ($S\cdots Cl = 3.183(2)$ Å), which results in the formation of an α-type network mediated by intermolecular $Pt\cdots S(O)_2\cdots Cl$ bonds (Fig. 6). Similar intermolecular interactions have been recognised earlier as an inorganic synthon for crystal engineering[34] and have also been established in the crystal structure of the hydroxy-substituted complex **2**. Note that in **2**, these interactions are responsible for the formation of β-type networks by cross-linking the $Pt–Cl\cdots H–O$ hydrogen bonding chains. Detailed examination of the crystal structures of the related bromide and iodide analogues, *viz*. the adducts **7**[29] and **8**, did not reveal any short intermolecular contacts between the metal-bound halide and the sulfur atom of a SO_2 molecule.

Finally, it should be noted that all the structures of the adducts are remarkably different from those of the corresponding SO_2-free analogues (*e.g.*, unit cell parameters, Table 1), even though the molecular (but not the atomic) content of the unit cell is conserved. The modifications are particularly obvious in the cases where the crystal system or the space group of the adduct is different from the parent SO_2-free complex (*cf.* the change of the crystal systems from monoclinic in **3** (X = Cl, R = H) and **5** (X = I, R = H) to orthorhombic in **6** and **8**, respectively).

Reactivity of arylplatinum complexes 3–8 in the solid phase

The solid-state reactivity of the complexes **3**–**5** has been verified by exposing the solid material (either crystalline or amorphous[35]) to a pure SO_2 atmosphere (1 atm). This caused an immediate colour change of the solid to orange, which indicates at least the *adsorption* of the gas, that is SO_2 fixation by the platinum centres located on the surface. Detailed analyses of these reactions by powder X-ray diffraction techniques provided unequivocal evidence for the formation of crystalline products in all cases, when the starting materials were crystalline as well. Exposure of the complexes **3**–**5** to SO_2 changes the diffraction patterns of the material completely and this clearly confirms that the reaction has taken place also in the interior of the crystalline substance, *i.e.*, SO_2 gas has been *absorbed* and is bound to the platinum center. The identification of the crystalline products as the corresponding SO_2 adducts **6**–**8**, respectively, has been performed by comparing the measured powder X-ray difractograms with the patterns calculated from the data available from single crystal diffractions, which provides an excellent fit. When exposed to air, the complexes **6**–**8** gradually lose their orange colour, which is indicative for the formation of the SO_2-free species **3**–**5**, respectively. The complexes have been obtained in crystalline form as well and therefore can undergo again another solid-state reaction, when exposed to an atmosphere containing SO_2 gas. Similar to the transformation of **1** to **2** and *vice versa*, gas binding and release may be repeated several times without significant loss of activity or crystallinity of the arylplatinum materials. This strongly points to processes which are fully reversible in all complexes **3**–**8**.[36]

Inclusion of guest molecules has been thoroughly investigated in recent years and particularly solvent molecules are well illustrated as guests.[37] Host–guest interactions at the gas–solid interface are rare and have been restricted predominantly to host matrices containing channel-like voids. Remarkably, the inclusion of gaseous SO_2 into arylplatinum solids induces a change of the net atomic content of the unit cell of the crystalline material and therefore an expansion and shrinking of the unit cell of up to 18% (corresponds to 232.1(3) $Å^3$ in the case of **3/6**) with the unique feature that both starting materials

Table 3 Crystallographic data for complexes **3**, **6** and **8**

	3 (X = Cl)	**6** (X = Cl)	**8** (X = I)
Empirical formula	$C_{12}H_{19}ClN_2Pt$	$C_{12}H_{19}ClN_2O_2PtS$	$C_{12}H_{19}IN_2O_2PtS$
Formula weight	421.83	485.89	577.34
T/K	200	150	150
Crystal system	Monoclinic	Orthorhombic	Orthorhombic
Space group	$P2_1/c$ (No. 14)	$Pna2_1$ (No. 33)	$Pbca$ (No. 61)
Crystal size/mm	0.50 × 0.30 × 0.13	0.25 × 0.19 × 0.05	0.20 × 0.20 × 0.08
Crystal colour	Colourless	Orange	Orange
a/Å	12.9877(14)	16.7796(1)	8.0291(9)
b/Å	9.2177(6)	10.0141(1)	15.1212(13)
c/Å	11.6041(12)	9.0940(1)	25.985(4)
β/°	111.104(8)		
V/Å^3	1296.0(2)	1528.09(2)	3154.8(7)
Z	4	4	8
D_{calc}/g cm^{-3}	2.162	2.112	2.431
μ/mm^{-1} (Mo-Kα)	11.008	9.493	10.984
Reflections measured, unique	6214, 2963	24501, 3499	7116, 3623
R_{int}	0.072	0.078	0.066
R_1[a] obs./all reflections	0.0247/0.0294	0.0210/0.0214	0.0413/0.0815
wR_2[b] all reflections	0.0506	0.0531	0.0752

[a] $R_1 = \Sigma||F_o| - |F_c||/\Sigma|F_o|$, for all $I > 2\sigma(I)$. [b] $wR_2 = [\Sigma[w(F_o^2 - F_c^2)^2]/\Sigma[w(F_o^2)^2]]^{1/2}$.

and products are crystalline. Note that the packing indices and hence the density are hardly changed upon adduct formation (Table 1).

Obviously, such organoplatinum self-assemblies may find application as solid-state sensors for the selective recognition of SO_2 gas,[38] which is indicated by unique and reversible modifications of the crystalline material which is accompanied by a colour change. Importantly, these arylplatinum species also display several characteristics desired for ideal gas storage systems, as they exert a high stability and no detectable loss of activity.[39] The detailed understanding of the fully characterised supermolecular nanosize carrier-systems allows the study of these gas uptake and release processes on a molecular level. This methodology may further lead to the property-directed design and construction of gas storage systems for application purposes.

On the supramolecular level, this reversible binding and release of SO_2 is accompanied by considerable modifications of the intermolecular architecture, since gas fixation and release cause a change in the atomic content of the unit cell and induce a re-orientation of the molecular arrangement. Hydrogen bonding has been accepted as a powerful tool for promoting the self-assembly of molecular units into a supramolecular array (*e.g.* a supermolecule).[3,10] Despite the absence of structural features that could direct such a self-assembly, the arylplatinum complexes **3**–**8** readily undergo crystalline transformations. Obviously, the hydrogen bonding motif present in **1** and **2** is an interesting but not an essential feature for the occurrence of these unique processes.

Conclusions

Crystalline arylplatinum complexes [PtX(NCN–R)], which display a closed structure, have been discovered to undergo a solid-state reaction with gaseous SO_2. This leads to the formation of adducts which are also crystalline and hence includes an increase of the atomic content in the unit cells. These transformations are reversible and upon release of SO_2 gas, the unit cell volume is reduced again to the initial volume. Notably, no special intermolecular network formation (either of α- or β-type) is required for this unique formation of crystalline products from arylplatinum complexes upon the binding or release of SO_2.

The remarkable expansion and shrinking processes are likely to involve local solutions of a small amount of the arylplatinum complex in SO_2 (or *vice versa*). Provided that this process is occurring randomly and in a time window of perhaps seconds, it will occasionally lead to a transfer of SO_2 from the interior of the solid material to the surface and finally to the atmosphere. Hence, the fixation and release of SO_2 is anticipated to take place in the temporarily and very locally formed solute within the crystalline material. This implies that in these materials (re-)crystallisation is an event which is comparable in rate to solute formation, since the overall crystallinity of the material is conserved (*cf.* time-resolved powder X-ray diffraction). Moreover, this process is proposed to occur in strictly localised manner and at low concentration levels and therefore is difficult to observe.

Consequently, these arylplatinum species represent a novel type of functional material for crystal engineering and the processing of crystalline solids. The full reversibility of SO_2 binding and release in these organoplatinum materials without loss of crystallinity suggests an application potential both as efficient sensors and as versatile crystalline switches. The 'on' and 'off' position of these switches can be detected by a variety of techniques such as UV-vis, IR spectroscopy, and powder X-ray diffraction. The conservation of supramolecular connectivities (such as the O–H · · · Cl–Pt hydrogen bonding) during these solid-state reactions is particularly attractive with respect to (opto-) electronic applications, where a high degree of regularity and ordering is essential.

Experimental

Materials

Gaseous SO_2 was purchased from Aldrich (99.9% purity) and used as received. The preparation of the arylplatinum complexes **1**–**8** has been described elsewhere.[19,21,28] The material was obtained in crystalline form by liquid–liquid diffusions of saturated solutions using DMSO–pentane (**1**), CH_2Cl_2–SO_2–hexane (**2** and **6**–**8**) or CH_2Cl_2–hexane (**3**–**5**) as solvents.

IR spectroscopy

FT-IR spectra were recorded with CaF_2 samples on a Perkin-Elmer system 2000 spectrometer (reflection mode) which was equipped with either a variable temperature sample unit or with an environmental DRIFT chamber (for sample exposure to SO_2 gas).

Powder X-ray diffraction

Powder X-ray diffraction intensities were measured from samples which were mounted in an open glass capillary on a

Nonius KappaCCD diffractometer with Cu-Kα radiation, graphite monochromator, $\lambda = 1.5418$ Å at a temperature of 293 K. Scans were performed every hour with a scan time of 6 minutes. The images were evaluated using locally written software. A background correction was applied prior to intensity determination.

Single crystal X-ray diffractions

Intensities were measured on an Enraf-Nonius CAD4-T (**3** and **8**) or a Nonius KappaCCD (**6**) diffractometer with a rotating anode (Mo-Kα, $\lambda = 0.71073$ Å). Crystal data and details on data collection and refinement are collected in Table 3. The structures were solved with Patterson methods (DIRDIF-97[40]) and refined against F^2 of all reflections (SHELXL-97[41]). Non-hydrogen atoms were refined freely with anisotropic displacement parameters, hydrogen atoms were refined as rigid groups. Weights were introduced in the last refinement cycles. Neutral atomic scattering factors and anomalous dispersion corrections were taken from the International Tables of Crystallography.[42] All calculations, graphical illustrations and checking for higher symmetry were performed with the PLATON[43] package.

CCDC reference number 186/2143.

See http://www.rsc.org/suppdata/dt/b0/b006419j/ for crystallographic files in .cif format.

Acknowledgements

We thank Professor van der Maas for fruitful discussions. This work was supported in part (A. L. S. and M. L.) by the Dutch Council for Chemical Sciences (CW-NWO).

References

1 (*a*) C. P. Collier, E. W. Wong, M. Belohradsky, F. M. Raymo, J. F. Stoddart, P. J. Kuekes, R. S. Williams and J. R. Heath, *Science*, 1999, **285**, 391; (*b*) M. A. Fox, *Acc. Chem. Res.*, 1999, **32**, 201.

2 (*a*) T. R. Kelly, H. De Silva and R. Silva, *Nature*, 1999, **401**, 150; (*b*) N. Koumura, R. W. J. Zijlstra, R. A. van Delden, N. Harada and B. L. Feringa, *Nature*, 1999, **401**, 152; (*c*) V. Balzani, M. Gómez-López and J. F. Stoddart, *Acc. Chem. Res.*, 1998, **31**, 405; (*d*) J.-P. Sauvage, *Acc. Chem. Res.*, 1998, **31**, 611; (*e*) T. R. Kelly, I. Tellitu and J. P. Sestelo, *Angew. Chem.*, *Int. Ed. Engl.*, 1997, **36**, 1866.

3 J. D. Dunitz, in *Perspectives in Supramolecular Chemistry. The Crystal as a Supramolecular Entity*, ed. G. R. Desiraju, Wiley, Chichester, 1996.

4 (*a*) G. R. Desiraju, *Crystal Engineering; The Design of Organic Solids*, Elsevier, Amsterdam, 1989; (*b*) *Perspectives in Supramolecular Chemistry. The Crystal as a Supramolecular Entity*, ed. G. R. Desiraju, Wiley, Chichester, 1996.

5 M. Hargittai and I. Hargittai, *Advances in Molecular Structure Research*, JAI Press, Greenwich, 1996.

6 (*a*) A. Gavezzotti, *Acc. Chem. Res.*, 1994, **27**, 309; (*b*) J. Maddox, *Nature*, 1988, **335**, 201; (*c*) J. J. Wolff, *Angew. Chem.*, 1996, **108**, 2339; J. J. Wolff, *Angew. Chem.*, *Int. Ed. Engl.*, 1996, **35**, 2195; (*d*) J. Pillardy, R. J. Wawak, Y. A. Arnautova, C. Czaplewski and H. A. Scheraga, *J. Am. Chem. Soc.*, 2000, **122**, 907; (*e*) W. T. M. Mooij, B. P. van Eijck and J. Kroon, *J. Am. Chem. Soc.*, 2000, **122**, 3500.

7 (*a*) B. H. Lipshutz, *Synthesis*, 1987, 325; (*b*) S. H. Bertz, *J. Am. Chem. Soc.*, 1990, **112**, 4031; (*c*) J. P. Snyder, D. P. Spangler and J. R. Behling, *J. Org. Chem.*, 1994, **59**, 2665; (*d*) C. M. P. Kronenburg, J. T. B. H. Jastrzebski, A. L. Spek and G. van Koten, *J. Am. Chem. Soc.*, 1998, **120**, 9688.

8 (*a*) J. D. Dunitz and J. Bernstein, *Acc. Chem. Res.*, 1995, **28**, 193; (*b*) S. Isz, I. Weissbuch, K. Kjaer, W. G. Bouwman, J. Als-Nielsen, S. Palacin, A. Ruaudel-Texier, L. Leiserowitz and M. Lahav, *Chem. Eur. J.*, 1997, **3**, 930.

9 M. J. Zaworotko, *Nature*, 1997, **386**, 220.

10 (*a*) J.-M. Lehn, *Angew. Chem.*, 1990, **102**, 1347; J.-M. Lehn, *Angew. Chem.*, *Int. Ed. Engl.*, 1990, **29**, 1304; (*b*) J.-M. Lehn, *Supramolecular Chemistry: Concepts and Perspectives*, VCH, Weinheim, 1995; (*c*) *Comprehensive Supramolecular Chemistry*, eds. J. L. Atwood, J. E. D. Davies, D. D. MacNicol and F. Vögtle, Pergamon Press, Oxford, 1996. For recent examples concerning hydrogen bonding for the self-assembly of molecular building blocks, see *e.g.* (*d*) L. J. Prins, J. Huskens, F. de Jong, P. Timmerman and D. N. Reinhoudt, *Nature*, 1999, **398**, 498; (*e*) P. Brunet, M. Simard and J. D. Wuest, *J. Am. Chem. Soc.*, 1997, **119**, 2737; (*f*) A. D. Burrows, C.-W. Chan, M. M. Chowdry, J. E. McGrady and D. M. P. Mingos, *Chem. Soc. Rev.*, 1995, 329; (*g*) J. C. MacDonald and G. M. Whitesides, *Chem. Rev.*, 1994, **94**, 2383.

11 (*a*) G. R. Desiraju, *Angew. Chem.*, 1995, **107**, 2541; G. R. Desiraju, *Angew. Chem.*, *Int. Ed. Engl.*, 1995, **34**, 2311; (*b*) D. Braga, F. Grepioni and G. R. Desiraju, *Chem. Rev.*, 1998, **98**, 1375; (*c*) D. Braga and F. Grepioni, *Chem. Commun.*, 1996, 571; (*d*) D. Braga and F. Grepioni, *Acc. Chem. Res.*, 1994, **27**, 51.

12 Y. Ohashi, K. Yanagi, T. Kurihara, Y. Sasada and Y. Ohgo, *J. Am. Chem. Soc.*, 1982, **104**, 5805.

13 P. J. Langley and J. Hulliger, *Chem. Soc. Rev.*, 1999, **28**, 279.

14 (*a*) M. Estermann, L. B. McClusker, C. Baerlocher, A. Merouche and H. Kessler, *Nature*, 1991, **352**, 320; (*b*) J. L. Meinershagen and T. Bein, *J. Am. Chem. Soc.*, 1999, **121**, 448.

15 (*a*) J. Hajdu, P. A. Machin, J. W. Campbell, T. J. Greenhough, I. J. Clifton, S. Zurek, S. Gover, L. N. Johnson and M. Elder, *Nature*, 1987, **329**, 178; (*b*) C. E. Buss, C. E. Anderson, M. K. Ponmije, C. M. Lutz, D. Britton and K. R. Mann, *J. Am. Chem. Soc.*, 1998, **120**, 7783.

16 See, *e.g.* (*a*) K. Novak, V. Enkelmann, G. Wegner and K. B. Wagener, *Angew. Chem.*, 1993, **105**, 1678; K. Novak, V. Enkelmann, G. Wegner and K. B. Wagener, *Angew. Chem.*, *Int. Ed. Engl.*, 1993, **32**, 1614; (*b*) J. R. Scheffer and P. R. Pokkuluri, in *Photochemistry in Organized & Constrained Media*, ed. V. Ramamurthy, VCH, New York 1990; for a few recent examples, see *e.g.* (*c*) K. Tanaka, H. Mizutani, I. Miyahara, K. Hirotsu and F. Toda, *Cryst. Eng. Comm.*, 1999, 3; (*d*) J. L. Foley, L. Li, D. J. Sandman, M. J. Vela, B. M. Foxman, R. Albro and C. J. Eckhardt, *J. Am. Chem. Soc.*, 1999, **121**, 7262; (*e*) S. Kobatake, M. Yamada, T. Yamada and M. Irie, *J. Am. Chem. Soc.*, 1999, **121**, 8450; (*f*) A. Matsumoto, T. Odani, M. Chikada, K. Sada and M. Miyata, *J. Am. Chem. Soc.*, 1999, **121**, 11122.

17 For other approaches, see *e.g.* (*a*) J. Aizenberg, A. J. Black and G. M. Whitesides, *Nature*, 1999, **398**, 495; (*b*) J. Aizenberg, A. J. Black and G. M. Whitesides, *J. Am. Chem. Soc.*, 1999, **121**, 4500; (*c*) K. Pohl, M. C. Bartelt, J. de la Figuera, N. C. Bartelt, J. Hrbek and R. Q. Hwang, *Nature*, 1999, **397**, 238.

18 (*a*) G. van Koten, *Pure Appl. Chem.*, 1989, **61**, 1681; (*b*) M. H. P. Rietveld, D. M. Grove and G. van Koten, *New J. Chem.*, 1997, **21**, 751.

19 P. J. Davies, N. Veldman, D. M. Grove, A. L. Spek, B. T. G. Lutz and G. van Koten, *Angew. Chem.*, 1996, **108**, 2078; P. J. Davies, N. Veldman, D. M. Grove, A. L. Spek, B. T. G. Lutz and G. van Koten, *Angew. Chem.*, *Int. Ed. Engl.*, 1996, **35**, 1956.

20 M. C. Etter, *J. Phys. Chem.*, 1991, **95**, 4601.

21 M. Albrecht, R. A. Gossage, M. Lutz, A. L. Spek and G. van Koten, *Chem. Eur. J.*, 2000, **6**, 1431.

22 Parts of this work have been communicated: M. Albrecht, M. Lutz, A. L. Spek and G. van Koten, *Nature*, 2000, **406**, 970.

23 A series of crystalline transformations involving a thermally induced shrinking process and hence no change in the atomic content of the unit cell has been reported recently: G. Ungar, V. Percec, M. N. Holerca, G. Johansson and J. A. Heck, *Chem. Eur. J.*, 2000, **6**, 1258.

24 L. Fabbrizzi, M. Licchelli and P. Pallavicini, *Acc. Chem. Res.*, 1999, **32**, 846.

25 In contrast to KBr, CaF_2 is inert toward SO_2 and therefore more appropriate as a carrier medium in solid-state IR. Anions of Br^- form adducts with SO_2 as well and therefore would remove this gas immediately from the eventually formed **2.** See, *e.g.* (*a*) D. F. Burow, *Inorg. Chem.*, 1972, **11**, 573; (*b*) E. J. Woodhouse and T. H. Norris, *Inorg. Chem.*, 1971, **10**, 614; (*c*) J. Jander and G. Tuerk, *Angew. Chem.*, 1963, **75**, 792; J. Jander and G. Tuerk, *Angew. Chem.*, *Int. Ed. Engl.*, 1963, **2**, 548.

26 (*a*) D. M. P. Mingos, *Transition Met. Chem.*, 1978, **3**, 1; (*b*) R. R. Ryan, G. J. Kubas, D. C. Moody and P. G. Eller, *Struct. Bonding* (*Berlin*), 1981, **46**, 47.

27 K. Moffat, *Acta Crystallogr.*, *Sect. A*, 1998, **54**, 833.

28 J. Terheijden, G. van Koten, F. Muller, D. M. Grove, K. Vrieze, E. Nielsen and H. C. Stam, *J. Organomet. Chem.*, 1986, **315**, 401.

29 W. J. J. Smeets, A. L. Spek, A. J. M. Duisenberg, J. A. M. van Beek and G. van Koten, *Acta Crystallogr.*, *Sect. C*, 1987, **43**, 463.

30 J. Terheijden, P. W. Mul, G. van Koten, F. Muller and H. C. Stam, *Organometallics*, 1986, **5**, 519.

31 S. L. James, G. Verspui, A. L. Spek and G. van Koten, *Chem. Commun.*, 1996, 1309.

32 J. P. Collman, L. S. Hegedus, J. R. Norton, R. G. Finke, *Principles and Applications of Organotransition Metal Chemistry*, University Science Books, Mill Valley, CA, 1987.

33 (*a*) M. Albrecht, R. A. Gossage, A. L. Spek and G. van Koten, *J. Am. Chem. Soc.*, 1999, **121**, 11898; (*b*) J. C. Muijsers, J. W. Niemantsverdriet, I. C. M. Wehman-Ooyevaar, D. M. Grove and G. van Koten, *Inorg. Chem.*, 1992, **31**, 26551; (*c*) R. A. Gossage, A. D. Ryabov, A. L. Spek, D. J. Stufkens, J. A. M. van Beek, van Eldik and G. van Koten, *J. Am. Chem. Soc.*, 1999, **121**, 2488.
34 M. Y. Darensbourg, T. Tuntulani and J. H. Reibenspies, *Inorg. Chem.*, 1995, **34**, 6287.
35 In the current context, we use the term amorphous to describe structures which are ordered up to the nanometer range (nanocrystalline), although this term ideally includes only completely randomly ordered structures. In contrast, micrometer and larger range ordered structures are referred to here as crystalline.
36 Time-dependent powder diffraction analyses on the transformation of **6** to **3** have shown that this process is linear in time, as previously established for the desorption of SO_2 from crystalline **2.**
37 (*a*) *Inclusion Compounds*, eds. J. L. Atwood, J. E. Davies and D. D. MacNicol, Academic, London, 1984, vols. 1–3; Oxford University Press, London, 1991, vols. 4–5; (*b*) T. Müller, J. Hulliger, W. Seichter, E. Weber, T. Weber and M. Wübbenhorst, *Chem. Eur. J.*, 2000, **6**, 54; (*c*) M. R. Caira, A. Coetzee, L. R. Nasimbeni, E. Weber and A. Wierig, *J. Chem. Soc.*, *Perkin Trans. 2*, 1997, 237.
38 M. Albrecht and G. van Koten, *Adv. Mater.*, 1999, **11**, 171.
39 (*a*) A. C. Dillon, K. M. Jones, T. A. Bekkedahl, C. H. Kiang, D. S. Bethune and M. J. Heben, *Nature*, 1997, **386**, 377; (*b*) P. Chen, X. Wu, J. Liu and K. L. Tau, *Science*, 1999, **285**, 91.
40 P. T. Beurskens, G. Admiraal, G. Beurskens, W. P. Bosman, S. Garcia-Granda, R. O. Gould, J. M. M. Smits and C. Smykalla, The DIRDIF Program System, Technical Report of the Crystallography Laboratory, University of Nijmegen, The Netherlands, 1997.
41 G. M. Sheldrick, SHELXL-97, Program for Crystal Structure Refinement, University of Göttingen, Germany, 1997.
42 D. T. Cromer, *International Tables for X-Ray Crystallography*, Kluwer, Dordrecht, 1990.
43 A. L. Spek, PLATON, a multipurpose crystallographic tool, Utrecht University, The Netherlands, 2000.